



## Serial in situ compression of spongiosa cylinder observed by $\mu$ CT, compared to simulated stress, strain, and movement

Bernhard Illerhaus<sup>1</sup>, E. Kunisch<sup>2</sup> and R. W. Kinne<sup>2</sup>

1 Bundesanstalt für Materialforschung und -prüfung (BAM), Germany,  
bernhard.illerhaus@bam.de

2 Experimental Rheumatology Unit, Department of Orthopedics, Jena University  
Hospital, Waldkliniken Eisenberg GmbH, Germany,  
Raimund.W.Kinne@med.uni-jena.de

### Abstract

Minimally invasive injection of calcium phosphate cement into bone defects in aged sheep vertebrae has been used as a model for the treatment of osteoporotic vertebral fractures (1). One of the therapeutic criteria is a compression test of non-treated or treated vertebral bodies. In the present study, an in situ compression test with a stepwise load increase was performed with small spongiosa cylinders from the vertebrae under continuous monitoring by  $\mu$ CT. This allows localization of bone cracks and the visualization of correct placement and form of the bone cylinder. In addition, the effects of an uneven load distribution on the sample due to an irregular shape and a subsequent underperformance of the test sample can be excluded by controlling its shape under increasing load. There was a good agreement between the measured data and those obtained by simulated load-dependent transformation on the basis of a digital volume correlation between consecutive compression tests on the bone surface under the assumption of homogeneous bone material. Mechanic simulation was executed by directly using structural voxel data, resulting in maps of Von Mises stresses and predicted displacements.

### 1. Introduction

The large animal model aged sheep (2) is used to test the regeneration of defined osteoporotic bone defects. Calcium phosphate cements containing reinforcing fibres and bone-inductive growth factors are injected to promote bone repair (3, 4). Time-dependent bone healing is non-destructively measured by x-ray and destructively assessed by biomechanical testing following excision of small bone sample. In the present study, spongiosa cylinders (diameter 10 mm; height 15 mm) were drilled out from the same position of different non-treated and treated vertebral bodies and tested for their compressive strength.

### 2. In situ CT

For the in situ inspection, a Deben 5000kN (5) stage was used. The total internal height was 50 mm, but the translation in compression mode was limited to 10 mm. Since the sample had a height of 15 mm, two acrylic glass spacers with a central, circular hole of 0.1 mm depth and 11 mm width were placed above and below the sample for fixation.



No damage occurred to the spacers during the tests. The spacers allowed the measurement of the sample height independently of the movement of the compression stage, since the x-ray transparent acrylic glass permits deduction of the respective sample height from the CT images. The compression stage was first slowly advanced (0.2 mm/s), until a force of 5 N was reached. This allowed a straight positioning of the sample and the measurement of a first tomogram. Since earlier tests had indicated the first occurrence of critical changes at loads above 800 kN, changes were measured at an intermediate load of 500 kN, then at 800 kN, and subsequently at increasing loads (step width 100 kN) until reaching the maximum load. This was done to avoid a compression of the samples to a height of  $\leq 2$  mm and unstable intermediate compression levels.

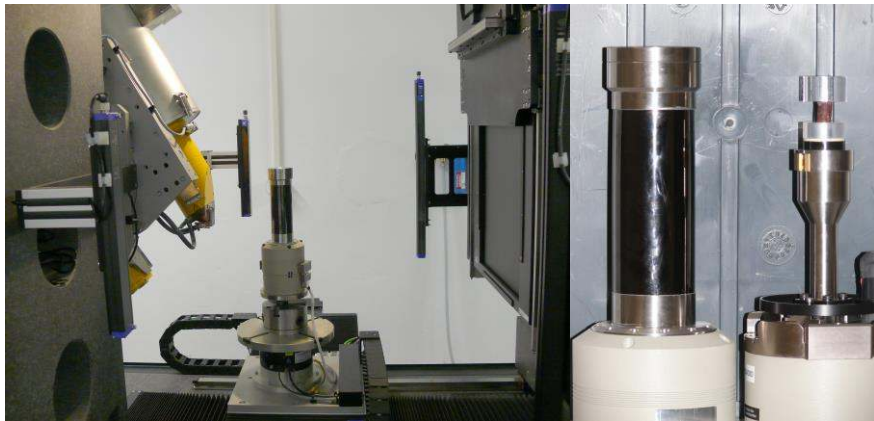


**Figure 1.** Left: Deben stage within CT system; measurements were performed as close as possible to the  $\mu$ CT tube. (Photo D. Meinel, BAM). Right: Deben 5000 N test rig; left: external load-bearing carbon fibre tube, right: open set-up with spongiosa cylinder and acrylic glass spacers.

Due to the large diameter of the Deben stage carbon tube in comparison to the sample diameter, the width of the 2 k pixel detector could only be partially used. The measurement parameters were: 100 kV, 160  $\mu$ A, no pre-filter and 1200 projections with 1 sec to 4 sec per shadow image. The source-to-detector distance was limited to 800 mm. The reconstructed images had a size of 999 x 999 x 1127 voxel with a side length of 15  $\mu$ m.

### 3. Samples and measurements

**Table 1. Samples and loads**

Sheep / vertebra	Image no. (bn)	Load / N
T18 / L1	0627-0635	20-1450
T18 / L2	0643-0649	20-1300
T18 / L3	0650-0657	20-1400
T18 / L4	0636-0642	25-1300
S59 / L1	0966-0971	5-993
S59 / L2	0950-0955	5-1000
S59 / L3	0956-0965	5-1276
S59 / L4	0972-0981	5-1550

In total, eight spongiosa cylinders from two sheep were measured. After the sample had been placed in the chamber, an initial contact load of 5-20 N was applied. Since a maximum load above 1000 N was expected, the subsequent steps were 500 N, 800 N, and further steps of 100 N. Table 1 gives the maximum load for each vertebra (and the corresponding CT-image numbers). The load and the displacement of the lower jaw were recorded by the Deben stage. The total time per CT could be reduced to 20 min without losing significant information by reducing the time per CT shadow image from 3 sec to 1 sec.

Although all samples were drilled out from different size vertebra, their structure was quite similar, with a homogeneous distribution of the bone material in the lower part and a hole due to a blood vessel in the upper part. The calculation of the density per slice in the CT image (perpendicular to the height) resulted in an overall density without significant variations (6). A vertical cut through a sample with the typical, cylindrical blood vessel channel is shown in Figure 2. At the lower end of the samples, white arrows indicate bone cracks occurring under increasing load.

In some of the samples, cracking occurred in the bone parts directly adjacent to the jaws, even at the intermediate load of 500 N. In the second campaign (S59), therefore, a sphere-balanced support plate was introduced below the sample. To test the effects of this modification, vertebra S59 / L1 was cut with an inclination of three degrees on the upper end and overshooting bone parts from the sampling process on the lower end. Although this modification was only performed in a low number of samples, it resulted in maximum loads quite comparable to those in the vertebra L2 without irregularities.

Additional calculations were performed on the basis of the in-situ CT images. For the samples of S59 the total bone mass per horizontal slice in relationship to the sample height was calculated. The four samples of S59 showed a good correlation between the maximum load and the respective bone mass (6).

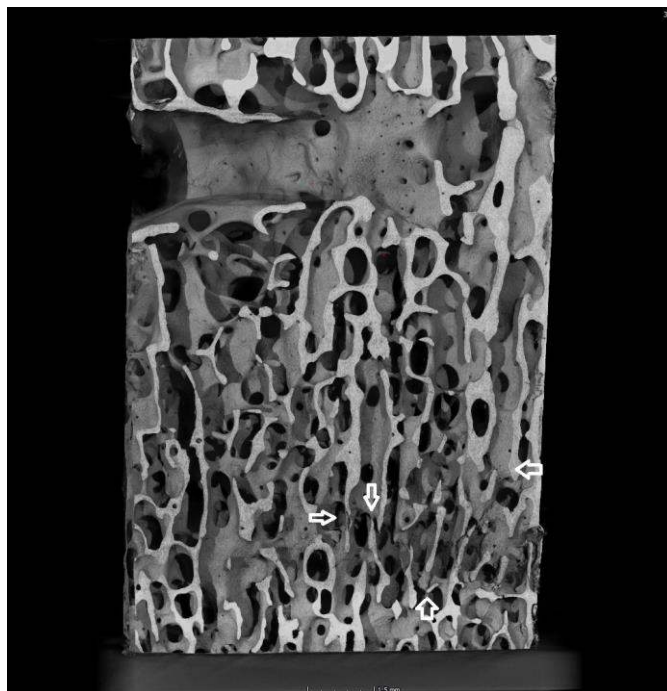


**Figure 2. Sample T18 / L1 (0634); last load step before severe destruction; arrows indicate the location of several cracks.**

#### 4. Compression, dislocation, simulation

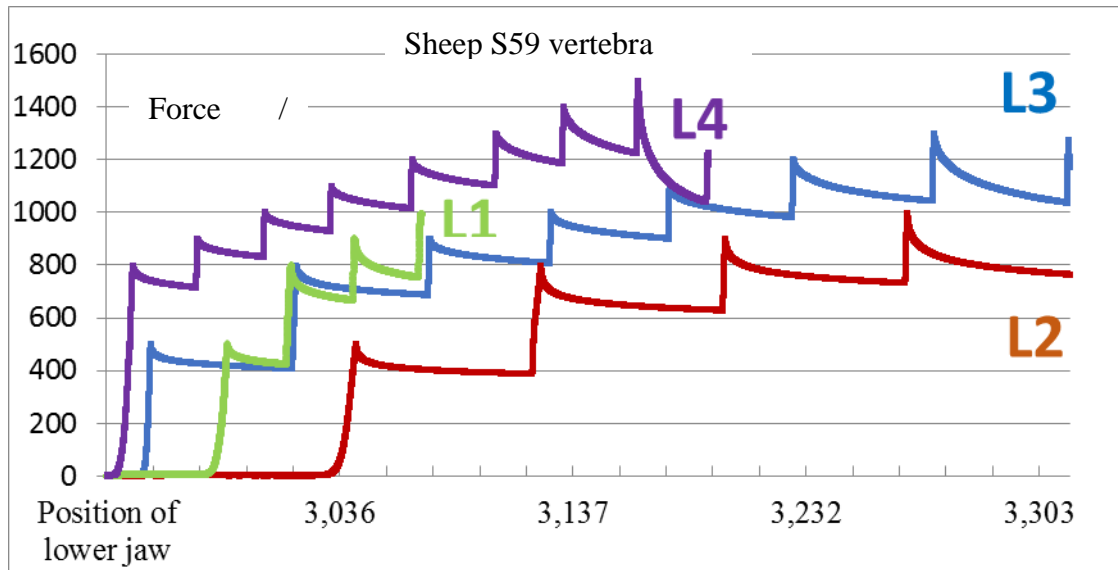


Figure 3. Sheep S59; L1-4 load diagrams; horizontal axes showing the position of the lower jaw (without movement during the acquisition of the CT; CT time between 20 min and 60 min).

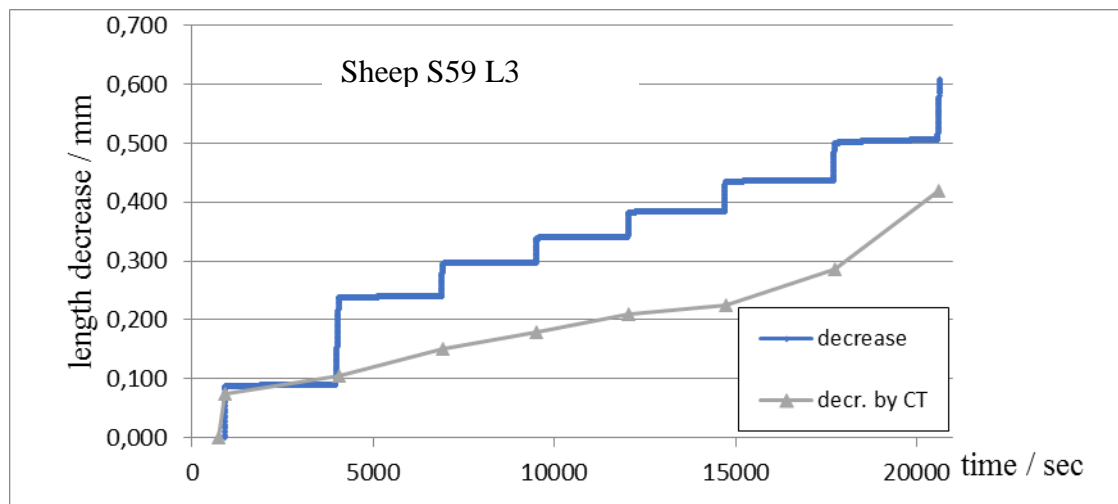


Figure 4. Sheep S59; L3 force-length-time diagram of vertebra L3; comparative measurement of the length decrease on the basis of the jaw displacement or the CT images.

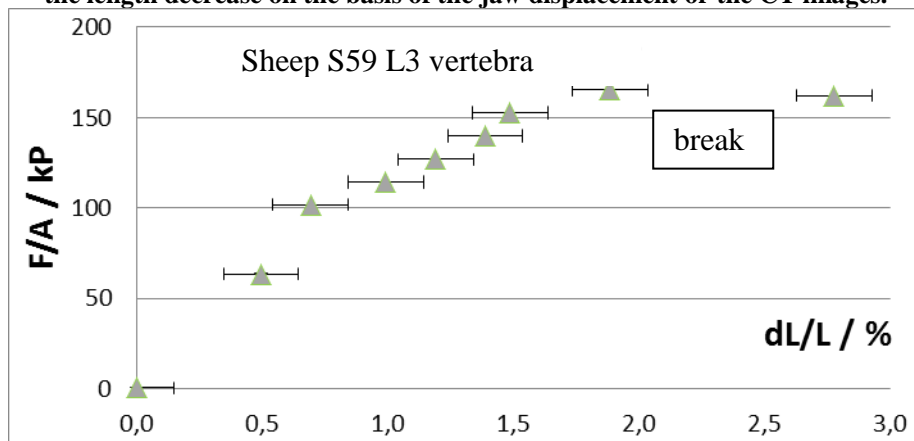
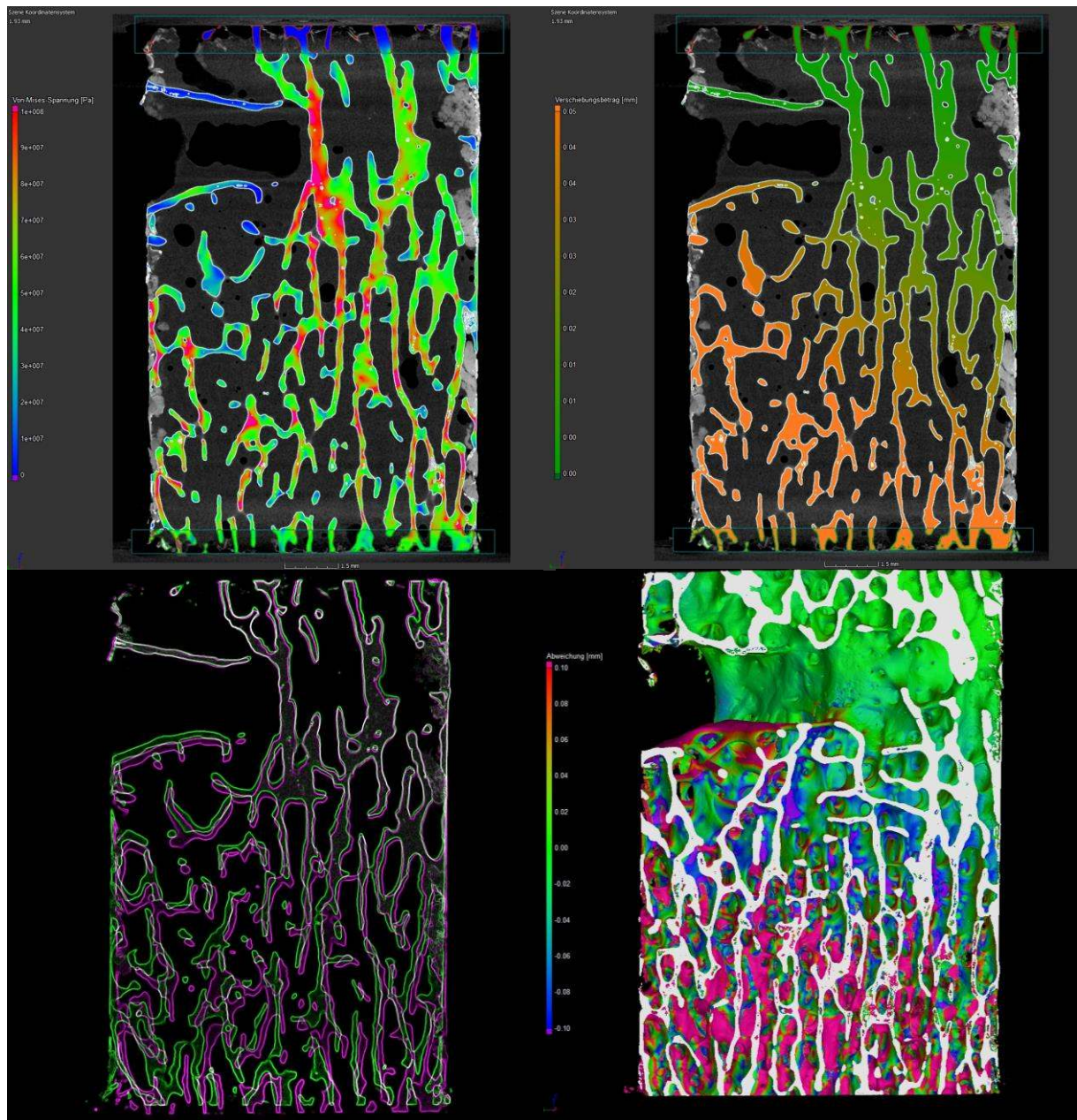
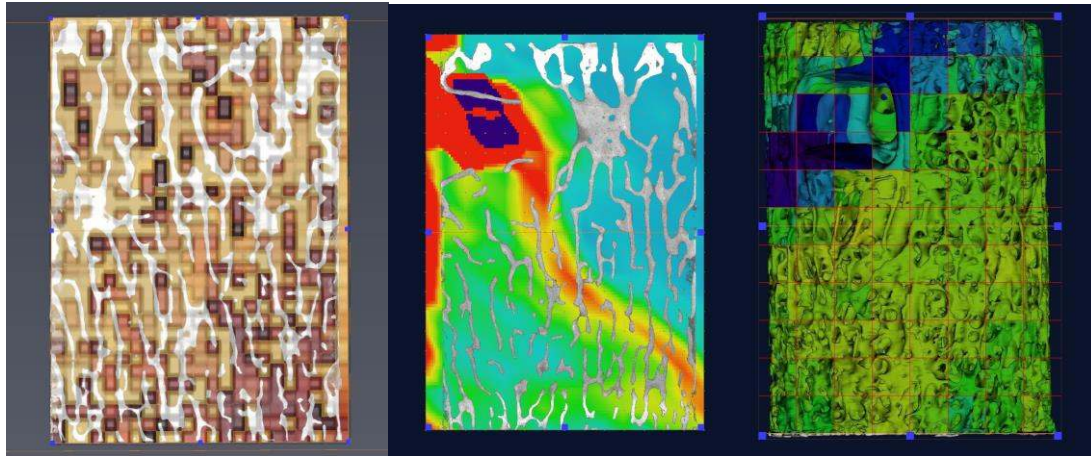


Figure 5. Sheep S59 vertebra L3 Stress / strain curve from CT images



**Figure 6. Image processing; top left: simulated maximal (red) and minimal load (blue); top right: simulated movement calculated from the load differences (see scale). Bottom left: contour comparison of first and last measurement; bottom right: calculated shift between first and last measurement.**



**Figure 7. Image processing; left: calculated shift upon maximal load by comparison of first and last measurement; dark brown - high value; middle: simulation of stress; right: shift calculated from the sample shown in the middle image (AVIZO DVC add on).**

Figure 3 displays the force-jaw movement curves of the compression tests for the four vertebrae L1 to L4 of sheep S59. During this measurement sequence, the total time for the acquisition of each individual CT was reduced to 20 min, since a good quality of the image was obtained and the bone surface could be generated with a high accuracy and without deviations.

In Figure 4 the graph is limited to the data of L3, but the length decrease was simultaneously calculated from the jaw displacement and the CT image. At 800 N (0.1 mm; 4000 sec), a difference developed between the results of the two calculations, which remained until sample failure. This suggests that full contact between sample and jaws is only established after reaching this point and emphasizes the importance of in situ CT during the biomechanical evaluation.

A stress-strain curve was also plotted for the L3 CT data (Figure 5). The data show error bars, because the upper and lower both ends of the sample can only be measured with an uncertainty of 1 pixel or 0.015mm. After omitting the first and last data point, a straight line with a defined slope could be calculated, allowing calculating and comparing the elasticity modulus of non-treated and treated bone samples.

In the present study, four different programs were applied to calculate the digital volume correlation (DVC), a pivotal parameter for in-situ experiments. The results of two programs are shown in this publication, one program has been used for the analysis of a different material, and the fourth program will be published in a PhD thesis (7).

One crucial point in DVC is the size and maximum number of volume packages which can be included in the analysis. Also, required calculation time and computer memory may be an issue. In most cases, a continuous behaviour of the material is assumed. For a brittle material (e.g., concrete) and a given image size of 1 k<sup>3</sup>, one thousand points of calculation will yield a smooth, but incorrect result. The present study deals with a highly structured sample containing more void than material, which generates technical problems for the DVC, since large parts of the volume packages contain no material. The same would apply to a less structured sample. Two potential approaches to this problem are: i) reduction of the difference of volume packages for the two states; ii) initiation from (iso)surface(s) and measurement of the distance to the relocated surface.

The second row of Figure 6 shows the comparison between starting state and maximum load for L1 of T18, as calculated with VGStudioMax (nominal-actual-comparison).

Notably, in the bottom right image the bottom of the blood vessel channel appears to move up (red), whereas the vertical wall remains unchanged (green). In the bottom left image, comparison of the contours of a vertical slice of the two states suggests a movement of the bottom part to the left. A simulation of the load distribution on the basis of the original CT using VGStudioMax yields very similar results (Figure 6 top left), especially concerning the area of displacement (Figure 6 top right, see scale). Despite the low number of samples currently analyzed, two types of failure mechanisms can thus be hypothesized, which depend on the bone density: i) in areas of low bone density, the blood vessel channel has a major influence; ii) in areas of high bone density, bone will fail in the midrange height (6).

Figure 7 shows the results applying the AVIZO DVC, which uses small sub-volumes to calculate the deviation. The left image (vertical cut containing deviations and sub-volumes) shows numerous sub-volumes located in void areas, as indicated by dark brown among ochre-coloured volumes in the upper sample. Interpolation of these values would result in averaged values, which may be incorrect. Enlargement of the sub-volumes may yield a better overall fit, but treats the sample as a continuous matter.

## 5. Conclusions

In-situ CT of bones during a stress test may reveal unwanted effects. The addition of a spherical axial support plate (SAM-12, igubal, igus GmbH, Köln) for the compensation of un-even top and bottom surfaces results in higher maximal loads. The tested DVC programs should be optimized, especially concerning the evaluation of highly structured material by the sub-volume method. However, simulations directly based on CT data already yield good predictions of the measured data.

## References

1. S Maenz et al., "Enhanced bone formation in sheep vertebral bodies after minimally invasive treatment with a novel, PLGA fiber-reinforced brushite cement." *The spine journal* 17, pp. 709-719, 2017.
2. M Bungartz et al. "First-time systematic postoperative clinical assessment of a minimally invasive approach for lumbar ventrolateral vertebroplasty in the large animal model sheep", *The Spine Journal*, Vol. 16, pp. 1263-1375, 2016.
3. L Xin et al. "Decreased extrusion of calcium phosphate cement versus high viscosity PMMA cement into spongy bone marrow—an ex vivo and in vivo study in sheep vertebrae", *The Spine Journal*, Vol. 16. 2016, pp. 1468-1477.
4. M Bungartz et al. "GDF5 significantly augments the bone formation induced by an injectable, PLGA fiber-reinforced, brushite-forming cement in a sheep defect model of lumbar osteopenia", *The Spine Journal*, Vol. 17. 2017, pp. 1685-1698.
5. Deben
6. B Illerhaus, E Kunisch, R W Kinne, Proceedings of the DGZfP Jahrestagung 2018, "µCT begleitete in-situ Druckversuche an spongiosen Knochen, Bestimmung des experimentellen und simulierten Verschiebungsfeldes, sowie der simulierten, internen Spannung.", to be published.
7. B Powierza, (PhD thesis, BAM, 2018) L Stelzer, T. Oesch, F Weise, G Bruno "Water Migration in One-Side Heated Concrete: 4D In-Situ CT Monitoring of the Moisture-Clog-Effect", to be published in: *Journal of Nondestructive Evaluation (JONE)*.